



**HAL**  
open science

## Physicochemical and Pharmacokinetic Profiles of Gadopiclesol. A New Macrocyclic Gadolinium Chelate With High T1 Relaxivity

Caroline Robic, Marc Port, Olivier Rousseaux, Stéphanie Louguet, Nathalie Fretellier, Sarah Catoen, Cécile Factor, Soizic Le Greneur, Christelle Medina, Philippe Bourrinet, et al.

► **To cite this version:**

Caroline Robic, Marc Port, Olivier Rousseaux, Stéphanie Louguet, Nathalie Fretellier, et al.. Physicochemical and Pharmacokinetic Profiles of Gadopiclesol. A New Macrocyclic Gadolinium Chelate With High T1 Relaxivity. *Investigative Radiology*, 2019, 54 (8), pp.475-484. 10.1097/RLI.0000000000000563 . hal-02311026

**HAL Id: hal-02311026**

**<https://cnam.hal.science/hal-02311026>**

Submitted on 10 Oct 2019

**HAL** is a multi-disciplinary open access archive for the deposit and dissemination of scientific research documents, whether they are published or not. The documents may come from teaching and research institutions in France or abroad, or from public or private research centers.

L'archive ouverte pluridisciplinaire **HAL**, est destinée au dépôt et à la diffusion de documents scientifiques de niveau recherche, publiés ou non, émanant des établissements d'enseignement et de recherche français ou étrangers, des laboratoires publics ou privés.



Distributed under a Creative Commons Attribution - NonCommercial - NoDerivatives 4.0 International License

## OPEN

# Physicochemical and Pharmacokinetic Profiles of Gadopiclesol A New Macrocyclic Gadolinium Chelate With High T1 Relaxivity

Caroline Robic, PhD,\* Marc Port, PhD,† Olivier Rousseaux, PhD,\* Stéphanie Louguet, PhD,\*  
Nathalie Fretellier, PhD,\* Sarah Catoen, PhD,\* Cécile Factor, PhD,\* Soizic Le Greneur, PhD,\*  
Christelle Medina, PhD,\* Philippe Bourrinet, PharmD,\* Isabelle Raynal, PhD,\*  
Jean-Marc Idée, PharmD, MS,\* and Claire Corot, PharmD, PhD\*

**Abstract: Objectives:** We aimed to evaluate gadopiclesol, a newly developed extracellular nonspecific macrocyclic gadolinium-based contrast agent (GBCA) having high relaxivity properties, which was designed to increase lesion detection and characterization by magnetic resonance imaging.

**Methods:** We described the molecular structure of gadopiclesol and measured the  $r_1$  and  $r_2$  relaxivity properties at fields of 0.47 and 1.41 T in water and human serum. Nuclear magnetic relaxation dispersion profile measurements were performed from 0.24 mT to 7 T. Protonation and complexation constants were determined using pH-metric measurements, and we investigated the acid-assisted dissociation of gadopiclesol, gadodiamide, gadobutrol, and gadoterate at 37°C and pH 1.2. Applying the relaxometry technique (37°C, 0.47 T), we investigated the risk of dechelation of gadopiclesol, gadoterate, and gadodiamide in the presence of ZnCl<sub>2</sub> (2.5 mM) and a phosphate buffer (335 mM). Pharmacokinetics studies of radiolabeled <sup>153</sup>Gd-gadopiclesol were performed in Beagle dogs, and protein binding was measured in rats, dogs, and humans plasma and red blood cells.

**Results:** Gadopiclesol [gadolinium chelate of 2,2',2''-(3,6,9-triaza-1(2,6)-pyridinacyclodecaphane-3,6,9-triyl)tris(5-((2,3-dihydroxypropyl)amino)-5-oxopentanoic acid); registry number 933983-75-6] is based on a pycn macrocyclic structure. Gadopiclesol exhibited a very high relaxivity in water ( $r_1 = 12.2 \text{ mM}^{-1}\cdot\text{s}^{-1}$  at 1.41 T), and the  $r_1$  value in human serum at 37°C did not markedly change with increasing field ( $r_1 = 12.8 \text{ mM}^{-1}\cdot\text{s}^{-1}$  at 1.41 T and  $11.6 \text{ mM}^{-1}\cdot\text{s}^{-1}$  at 3 T). The relaxivity data in human serum did not indicate protein binding. The nuclear magnetic relaxation dispersion profile of gadopiclesol exhibited a high and stable relaxivity in a strong magnetic field. Gadopiclesol showed high kinetic inertness under acidic conditions, with a dissociation half-life of  $20 \pm 3$  days compared with  $4 \pm 0.5$  days for gadoterate, 18 hours for gadobutrol, and less than 5 seconds for gadodiamide and gadopentetate. The pharmacokinetic profile in dogs was typical of extracellular nonspecific GBCAs, showing distribution in the extracellular compartment and no metabolism. No protein binding was found in rats, dogs, and humans.

**Conclusions:** Gadopiclesol is a new extracellular and macrocyclic Gd chelate that exhibited high relaxivity, no protein binding, and high kinetic inertness.

Its pharmacokinetic profile in dogs was similar to that of other extracellular nonspecific GBCAs.

**Key Words:** gadopiclesol, magnetic resonance imaging, GBCA, relaxivity, pharmacokinetics, gadolinium, physicochemistry

(*Invest Radiol* 2019;54: 475–484)

Thirty years after their introduction, it is indisputable that the use of nonspecific gadolinium-based contrast agents (GBCA) in neurological, spinal, abdominal, cardiac, and vascular magnetic resonance imaging (MRI) has substantial benefits for evidence-based disease management.<sup>1</sup> Notably, MRI with GBCA-based contrast enhancement is crucial for detecting small brain metastases.<sup>2</sup>

Metastatic brain lesions are, by far, the most common type of central nervous system (CNS) tumors in adults. Population-based studies indicate incidence rates ranging from 8.3 to 14.3 per 100,000 population, and brain metastases affect 8.5% to 9.6% of cancer patients. Moreover, these values are probably underestimated.<sup>3</sup> New imaging modalities are associated with a rising incidence of known CNS metastases.<sup>3</sup> Neuroimaging is highly dependent on GBCA administration, which dramatically improves CNS lesion detection and depiction, and thus facilitates diagnosis, sometimes enables determination of tumor grade and may guide the treatment.<sup>4</sup>

It was previously a common strategy to increase the GBCA dose to improve sensitivity during neuroimaging procedures.<sup>4</sup> Improved images can also be obtained by using both a higher GBCA dose and a higher magnetic field (3 T vs 1.5 T).<sup>5</sup> Gadolinium-based contrast agents were long considered one of the safest classes of drugs.<sup>6</sup> However, this perception changed in 2006 after reports that prior GBCA administration is causally linked to the seriously debilitating disease nephrogenic systemic fibrosis (NSF).<sup>7–9</sup> Further investigations revealed that NSF was specifically associated with the use of linear GBCAs.<sup>10,11</sup> Gadolinium-based contrast agents are classified as linear or macrocyclic agents based on the molecular structure of their polyazapolycarboxylic ligand.<sup>12</sup> Linear GBCAs are characterized by a lower kinetic stability than macrocyclic GBCAs.<sup>12</sup> Most pre-clinical studies performed in clinically relevant *in vivo* models support a causal role of linear but not macrocyclic GBCAs in NSF.<sup>13–16</sup>

The gradual dissociation of linear GBCAs has been observed *in vivo*,<sup>15,16</sup> and Gd versus endogenous metal transmetallation is proposed as a likely trigger of the proinflammatory and profibrotic pathways involved in NSF.<sup>17</sup> It was recently reported that repeated administrations of GBCAs (almost exclusively of the linear category) lead to accumulation in specific areas of the brain, mostly in the dentate nucleus and the globus pallidus, but also at other CNS sites after repeated administrations of linear GBCAs.<sup>18,19</sup> Biospeciation studies with linear GBCAs have concluded that the brain tissue contains multiple species of Gd—including chelated and soluble, dissociated and insoluble, and dissociated and soluble—which are likely macromolecule-bound.<sup>20–22</sup>

The European Union has suspended the use of all linear nonspecific GBCAs, except those dedicated to specific indications

Received for publication January 21, 2019; and accepted for publication, after revision, February 21, 2019.

From the \*Research and Innovation Division, Guerbet, Aulnay-sous-Bois; and †Laboratoire de Génétique, Bioinformatique et Chimie Moléculaire (EA 7528), Equipe Chimie Moléculaire, Conservatoire National des Arts et Métiers (CNAM), HESAM Université, Paris, France.

Conflicts of interest and sources of funding: All authors are or were employees of Guerbet. This work is part of the Franco-German Project ISEULT and was funded in part by Banque Publique d'Investissement (France) and by Guerbet.

Correspondence to: Jean-Marc Idée, PharmD, MS, Research and Innovation Division, Guerbet, BP 57400 Roissy-Charles de Gaulle Cedex, France. E-mail: jean-marc.idée@guerbet.com.

Copyright © 2019 The Author(s). Published by Wolters Kluwer Health, Inc. This is an open-access article distributed under the terms of the Creative Commons Attribution-Non Commercial-No Derivatives License 4.0 (CCBY-NC-ND), where it is permissible to download and share the work provided it is properly cited. The work cannot be changed in any way or used commercially without permission from the journal.

ISSN: 0020-9996/19/5408–0475

DOI: 10.1097/RLI.0000000000000563

(liver or joint imaging).<sup>23</sup> The US Food and Drug Administration (FDA) has also recognized that linear GBCAs are associated with greater retention for a longer duration compared with macrocyclic GBCAs, and has followed a different approach. The FDA states that healthcare professionals should consider the Gd-retention characteristics of each agent when choosing a GBCA for at-risk patients. The FDA has also requested that radiologists minimize repeated GBCA imaging studies when possible, particularly in closely spaced MRI investigations.<sup>24</sup>

Because procedures using high doses of existing GBCAs are less common, there is a need for new extracellular nonspecific GBCAs allowing detection of more metastatic lesions using high magnet fields and without increasing the dose.<sup>4</sup> One obvious way of dealing with this issue is to increase the longitudinal relaxivity of GBCAs to increase the contrast between the lesion and background healthy parenchyma with the classic dose of 0.1 mmol Gd/kg.<sup>25,26</sup> A sufficient relaxivity increase could even enable reduction of the Gd dose without lowering the current efficacy associated with extracellular and nonspecific GBCAs.<sup>4</sup> All extracellular GBCAs currently on the market have roughly similar relaxivity properties,<sup>27</sup> and their use at higher doses is limited due to potential safety concerns.

Gadopicolenol, a new macrocyclic GBCA characterized by a very high  $r_1$  relaxivity, is currently under development. In the present article, we aimed to summarize the chemical, physicochemical, and nonclinical pharmacokinetic data regarding gadopicolenol.

## MATERIALS AND METHODS

### Osmolality

The osmolality of a 10- $\mu$ L sample of gadopicolenol (0.5-M solution) was determined using a Vapro pressure osmometer (Wescor Inc, Logan, UT) pressure. Before each use, the osmometer was calibrated with 3 standards (Opti-Mole; 100, 290, and 1000 mOsm/kg H<sub>2</sub>O). Measurement was performed in triplicate.

### Viscosity

The viscosity was assessed using a Kinexus rotative rheometer (Malvern Panalytical SARL, Orsay, France) at 37°C. The gadopicolenol solution (0.5 M) was loaded between a 60-mm and 2-degree cone and plate. Stresses between 1 and 5 Pa were applied. For each stress, the resulting shear rate was measured. The slope of the curve stress as a function of shear rates gave the viscosity of the test sample.

### Log P Value (*n*-Octanol/Water)

Gadopicolenol was brought into solution in a 50/50 mixture of *n*-octanol and pH 7.4 phosphate-buffered saline. Mixture was maintained at 37°C during 24 hours under continuous stirring. Subsequently, the 2 phases were taken. Gadopicolenol concentration was then measured in both media by UHPLC (ultra-high-performance liquid chromatography) technique: UHPLC Waters using a column Cortecs T3 150  $\times$  2.1 mm, 1.6  $\mu$ m (Waters SAS, Guyancourt, France).

### Relaxivity Measurements at 20 and 60 MHz

The longitudinal relaxivity of the Gd chelate gadopicolenol was determined based on the spin lattice relaxation time (T<sub>1</sub>). T<sub>1</sub> was measured using Bruker Minispec mq20 and mq60 analyzers (Bruker Biospin, Wissembourg, France) operating at frequencies of 20 MHz (0.47 T) or 60 MHz (1.41 T). In water or human serum, we prepared gadopicolenol solutions at 6 Gd concentrations: 0.5, 1.0, 2.0, 3.0, 4.0, and 5.0 mM. T<sub>1</sub> measurements were performed for the 6 concentrations, using the standard inversion recovery pulse sequence (180°- $\tau$ -90°), with the temperature maintained at 37°C  $\pm$  0.1°C. T<sub>1</sub> was calculated from a monoexponential plot of time versus signal intensity. The longitudinal relaxivity was calculated from the slope of

the regression line obtained by plotting 1/T<sub>1</sub>-1/T<sub>1</sub>dia versus the concentration of the complex, using the least-squares fitting method.

We determined the transverse relaxation time (T<sub>2</sub>) using the standard Carr-Purcell-Meiboom-Gill pulse sequence (90°- $\tau$ -180°).<sup>28,29</sup> T<sub>2</sub> relaxation time was calculated from the exponential curve of time versus signal intensity, measured for 6 concentrations. The transverse relaxivity value was calculated from the slope of the regression line obtained by plotting 1/T<sub>2</sub>-1/T<sub>2</sub>dia versus the concentration of the complex, using the least-squares fitting method.

Error bars on the relaxivity data were estimated at  $\pm$ 6% via an internal study considering 9 independent samples with measurements performed by 3 experimenters (3 samples each) with Gd dosage via inductively coupled plasma-atomic emission spectroscopy of the highest concentrated samples (5 mM).

## Nuclear Magnetic Relaxation Dispersion Profile Measurements

Proton nuclear magnetic relaxation dispersion (NMRD) profiles were determined using a Stelar Spinmaster FFC fast-field-cycling NMR relaxometer (Stelar, Mede [PV], Italy) over a magnetic field strength range of 0.24 mT to 0.24 T. Measurements were performed using 0.6-mL samples in Pyrex tubes with a 10-mm optical dimension. We additionally obtained relaxation rates using Minispec relaxometers mq20 (20 MHz, 0.47 T) and mq60 (60 MHz, 1.41 T) and a Bruker AMX-300 spectrometer (300 MHz). Nuclear magnetic relaxation dispersion profiles were determined using Mons University equipment. Values at 3 T were extrapolated from NMRD profiles. Because these measurements were performed at only one concentration, the error bars were estimated at  $\pm$ 10% (internal study on 9 samples with 3 experimenters). Proton NMRD curves were fitted using data processing software that included various theoretical models describing nuclear relaxation phenomena.

## Thermodynamic Stability

For the determination of protonation and complexation constants, we performed pH-metric measurements using a thermoregularized cell (25°C  $\pm$  0.1°C). An argon stream was run over the solution to avoid carbon dioxide dissolution. We used a Metrohm type T glass microelectrode (Metrohm, Herisau, Switzerland) with a low alkaline error. The procedures and apparatus used for potentiometric measurements have been previously described.<sup>30</sup> The ionic product of water (pK<sub>w</sub> = 13.78, at 25°C  $\pm$  0.1°C in 0.1 M NMe<sub>4</sub>Cl) was determined from titrations of acetic acid with a CO<sub>2</sub>-free NMe<sub>4</sub>OH solution. The protonation constants of the gadopicolenol ligand were determined from 8 titrations, with ligand concentrations ranging from 1 to 5 mM in the presence of HCl.

We determined the gadopicolenol constant using 5 series of 40 solutions of Gd<sup>3+</sup> and ligand (with ligand concentrations of 7.6  $\times$  10<sup>-4</sup> mol/L to 1.15  $\times$  10<sup>-3</sup> mol/L) plus HCl. These solutions were prepared in stoppered flasks under argon. The total ligand quantity was always slightly greater than the Gd<sup>3+</sup> quantity to prevent precipitation of the hydroxide Gd(OH)<sub>3</sub>. The pH of the solutions was adjusted to values ranging from 2 to 8 by addition of a 5  $\times$  10<sup>-2</sup> M NMe<sub>4</sub>OH solution. After a 30-day stabilization period at 37°C, the solutions were maintained at 20°C for 1 day before pH measurement.

Protometric data were processed by using the PROTAF program<sup>31</sup> to obtain the best-fit chemical model and refined overall stability constants. The PROTAF program is based on the weighted least-squares of the residues of the experimental variables (volume of titrant, pH), and allows simultaneous processing of 10 titrations, each including 150 pairs of data (volume, pH).

All experiments were performed at Reims, France in the Institute of Molecular Chemistry.

## Kinetic Inertness in Acidic Medium

We investigated the acid-assisted dissociation of the Gd chelates (concentration of  $8 \times 10^{-6}$  M) in a hydrochloric acid solution (37°C, pH 1.2) under pseudo-first-order conditions without control of the ionic strength, by following Gd release in the solution. From an initial 150-mL solution, a 25-mL aliquot was withdrawn and mixed with 1 mL of Arsenazo III [2,2'-(1,8-dihydroxy-3,6-disulfonaphthylene-2,7-bisazo)bisbenzenearsonic acid, 2,7-bis(2-arsenophenylazo) chromotropic acid solution; concentration of  $5.3 \times 10^{-4}$  M] without any buffer addition. Fifteen minutes after mixing, spectrometric measurement was assayed at 654 nm in a 10-mm cell. This measurement was performed for each point (Fig. 3). We compared gadopiclenol with gadoterate meglumine (macrocylic GBCA, Dotarem 0.5 M; Guerbet, Villepinte, France), gadobutrol (macrocylic GBCA, Gadavist/Gadovist 1 M; Bayer, Berlin, Germany), and gadodiamide (linear GBCA, Omniscan 0.5 M; GE Healthcare, Chalfont St Giles, United Kingdom).

## Dechelation in the Presence of Phosphate and Zn<sup>2+</sup>

We added 5 mL of a 2.5-mM Gd chelate solution to 5 mL of a 2.5-mM ZnCl<sub>2</sub> solution, which were both freshly prepared in phosphate buffer (pH 7, 335 mM). Measurement of the relaxivity at T<sub>0</sub> of this mixture was performed extemporaneously. The mixture was then kept at 37°C. At various time-points, 330-μL aliquots were withdrawn and the T1 relaxation time was measured at 37°C. Relaxivity was measured at 20 MHz (ie. 0.47 T) using a Bruker Minispec mq20 instrument. Gadopiclenol was compared with gadoterate meglumine and gadodiamide.

## Pharmacokinetics Studies

Pharmacokinetic evaluation was performed using gadopiclenol radiolabeled with the gamma emitter <sup>153</sup>Gd. <sup>153</sup>Gd-gadopiclenol (stated radiochemical purity >98%, specific activity 10.39 mCi/mmol) was prepared by Chelatec SAS, Saint Herblain, France, as a solution at a concentration of 0.428 mmol Gd/mL. All samples were subjected to gamma counting for 1 mn using an automatic controlled gamma counter (Packard Cobra II Auto Gamma, PerkinElmer, Waltham, MA) with correction for background and counter efficiency. We acquired the total radioactivity and sample weight data using the Debra Management System, versions 5.2 and 5.7 (LabLogic Systems Limited, Sheffield, United Kingdom).

The regulations conformed to the European Convention for the Protection of Vertebrate Animals Used for Experimental and Other Scientific Purposes (Strasbourg, Council of Europe) and achieved the standard of care required by the US Department of Health and Human Services' Guide for the Care and Use of Laboratory Animals.

## Plasma Pharmacokinetics

We evaluated plasma pharmacokinetics in 3 male and 3 female Beagle dogs (age, 5–6 months; body weight, 7.4–10.5 kg; Charles River, Edinburgh, United Kingdom). Animals received an intravenous (IV) bolus injection (cephalic vein) of 0.2 mmol Gd/kg of <sup>153</sup>Gd-gadopiclenol. Blood samples were collected into heparinized tubes by jugular vein venipuncture at 5, 15, and 30 minutes, and 1, 2, 4, 6, 8, 24, and 48 hours postdose.

## Excretion

To assess gadopiclenol elimination, the animals were housed singly in stainless steel metabolism cages, specially designed for the quantitative collection of urine and feces. Except for a period of fasting from overnight predose to 4 hours postadministration, a daily allowance of 400 g of a standard laboratory diet of known formulation (Harlan Teklad Global Diet, code 2021C) and domestic mains tap water were

available ad libitum. Holding and study areas had automatic control of light cycles and temperature. Light hours were 7:00 AM to 7:00 PM. Ranges of temperature and humidity measured during the study were 20°C to 22°C and 24% to 50%, respectively. We administered <sup>153</sup>Gd-gadopiclenol intravenously to Beagle dogs (0.2 mmol Gd/kg; 3 males and 3 females). Urine was collected before IV administration, at 0 to 6 hours and 6 to 24 hours postdose, and then at 24-hour intervals up to termination at 168 hours. Feces were quantitatively collected predose, and then at 24-hour intervals up to termination. Cages were washed daily with water following each sample collection. Cage debris was collected at 168 hours. All samples were retained for analysis. Total radioactivity levels were measured in all collected samples. Urine and plasma samples were analyzed for potential metabolites by HPLC. High-performance liquid chromatography was conducted using an Agilent 1100 Series Liquid chromatograph radiodetector and Packard Model 150TR flow scintillation analyzer (Packard, Downers Grove, IL) at 4°C with a Symmetry C18 column.

## Pharmacokinetic Parameter Calculation

The concentration data from urine and plasma were used to calculate selected pharmacokinetic parameters with WinNonlin pharmacokinetic software, version 5.2.1 (Pharsight Corp, Sunnyvale, CA). We implemented a noncompartmental approach consistent with the IV bolus route of administration. Parameters were estimated using actual sampling times relative to the end of each dose administration. We calculated the area under the curve from the plot of plasma total radioactivity versus time, using the linear trapezoidal method with linear interpolation.

## Protein Binding

To evaluate the in vitro binding of <sup>153</sup>Gd-gadopiclenol to plasma proteins and blood cells of rats, dogs, and humans, we performed equilibrium dialysis at nominal concentrations of 0.01, 0.1, 1, and 5 μmol/mL (incubation in a water bath set to maintain a temperature of 37°C for 2 hours). After incubation, duplicate aliquots of each half-cell compartment were assayed for radioactivity to determine the plasma protein binding or association with blood cells.

## RESULTS

### Chemical Structure and Synthesis

Gadopiclenol (Guerbet, Villepinte, France, patent number EP 1931 673 B1, page 8, example 2) is a gadolinium chelate of 2,2',2''-(3,6,9-triaza-1(2,6)-pyridinacyclodecapane-3,6,9-triyl)tris(5-((2,3-dihydroxypropyl)amino)-5-oxopentanoic acid) (registry number 933983-75-6; Fig. 1). It has a pyclen-based macrocyclic structure that is highly stable in terms of Gd dissociation and exhibits high relaxivity due to improved water access to the Gd ion. Its molecular weight is 970.11 g/mol, when calculated without the 2 water molecules that coordinate in solution.

Pyclen (3,6,9-triaza-1(2,6)-pyridinacyclodecapane) (registry number 78668-34-5) was alkylated with 3 equivalent of diethyl 2-bromopentanedioate, and the obtained hexaester was saponified to generate the corresponding hexacarboxylic acid derivative. The polyacid was complexed with 1 equivalent of Gd (Gd<sub>2</sub>O<sub>3</sub>), and this complex was used in a peptidic coupling reaction with 3 equivalents of 3-aminopropane-1,2-diol to yield the desired hydrophilic and stable macrocyclic chelate.

The molecular structure (Fig. 1) exhibits 6 asymmetric centers that can display 64 stereoisomers in solution.

Gadopiclenol was designed to provide optimal properties regarding its application in MRI, especially in terms of efficacy and safety.

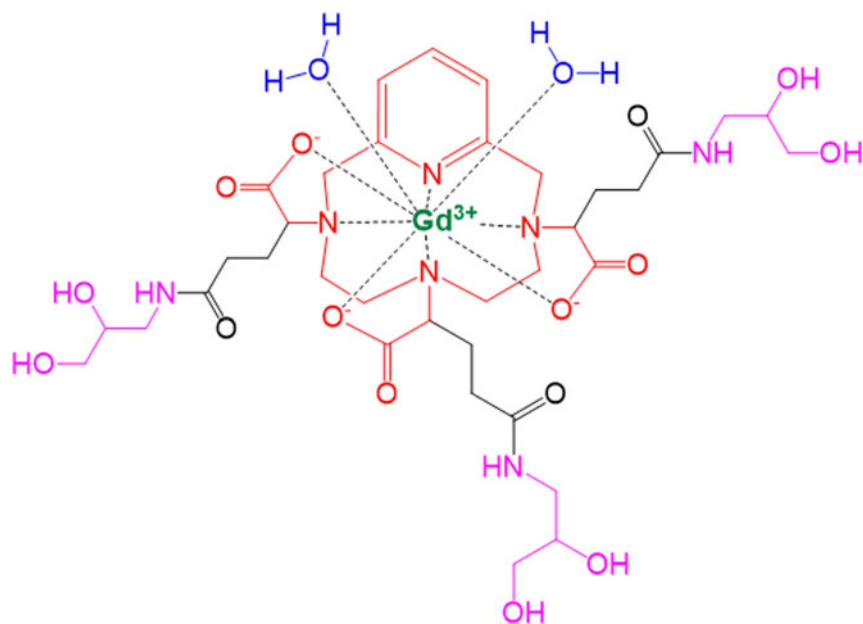


**FIGURE 1.** Chemical structure of gadopipiclenol [gadolinium chelate of 2,2',2''-(3,6,9-triaza-1(2,6)-pyridinacyclodecaphane-3,6,9-triyl)tris(5-((2,3-dihydroxypropyl)amino)-5-oxopentanoic acid)]. The PCTA parent structure is shown in red. Two water molecules are included to show the coordination in solution.

### Osmolality, Viscosity, and Hydrophilicity (Log *P* *n*-Octanol/PBS)

Gadopipiclenol exhibited an osmolality of 843 mOsm/kg H<sub>2</sub>O. Its log *P* value in *n*-octanol/PBS was of -4.2 and its viscosity was 7.6 mPa·s (Table 1).

### Relaxivity in Different Media

Relaxivity values of gadopipiclenol in water and in human serum at 3 different magnetic fields (0.47, 1.5, and 3 T) are displayed in Table 1. Gadopipiclenol exhibited a high *r*<sub>1</sub> relaxivity in water and human serum. The relaxivity data in human serum suggested no protein binding (Table 1).

### Thermodynamic and Conditional Constants

Gadopipiclenol conditional constant at pH 7.4 was calculated from the measured thermodynamic constant and from the 4 protonation constants of the ligand (Table 2).

### Nuclear Magnetic Relaxation Dispersion Profile

Gadopipiclenol exhibited an NMRD profile with a high relaxivity, which was stable at high clinical magnetic field (Fig. 2).

### Kinetic Stability Under Acidic Conditions

Experiments were performed using gadopipiclenol, gadoterate, gadobutrol, and gadodiamide at a highly acidic pH. Figure 3 shows the kinetics of dissociation of these Gd chelates. Gadopipiclenol exhibited the highest kinetic stability with a dissociation half-life of 20 ± 3 days at pH 1.2 (Table 1).

### Kinetic Dissociation in the Presence of Phosphate and Endogenous Cation (Zn<sup>2+</sup>)

In the presence of Zn<sup>2+</sup> and phosphate, gadodiamide exhibited a sharp decrease of the *r*<sub>1</sub>(t)/*r*<sub>1</sub>(t<sub>0</sub>) ratio. Conversely, the relaxivities of gadopipiclenol and gadoterate remained constant over the experimental period in the presence of Zn<sup>2+</sup> and phosphate (Fig. 4).

## Pharmacokinetics Studies

### Plasma Pharmacokinetics

Table 3 presents the main plasma pharmacokinetics parameters. Figure 5 shows the mean levels of total radioactivity in plasma after bolus administration of <sup>153</sup>Gd-gadopipiclenol in dogs. The highest mean plasma level of total radioactivity (*T*<sub>max</sub>) was observed at 5 mn postdose (first sampling). This level then showed a rapid biexponential decline over the first 24 hours postdose. No sex difference was found. The distribution volume was consistent with gadopipiclenol distribution within the extracellular water volume.

### Excretion

The major excretion route of total radioactivity was via urine. The mean percentages of administered radioactivity excreted by 168 hours postdose were 93.9% in urine and 5.7% in feces. Total excretion was rapid, with approximately 100% of the administered dose excreted during the first 24 hours postdose.

The recovery data from one female dog was excluded from the mean calculations due to the low recoveries in this animal. This might be due to loss of urine at collection as the low recovery was particularly evident in the first urine collection (0–6 hours).

### Metabolism

High-performance liquid chromatography analysis revealed the presence of only unchanged gadopipiclenol in plasma and urine samples.

### Protein Binding

Over the investigated concentration range (0.01–5 μmol/mL), we detected negligible binding of <sup>153</sup>Gd-gadopipiclenol to plasma proteins in all species (0% in rats, 1.4% in dogs, and 0.5% in humans), which was independent of the concentration. Binding of <sup>153</sup>Gd-gadopipiclenol to red blood cells was also low in all species (6%–16.7% in rats, 0%–3.2%

**TABLE 1.** Osmolality, Relaxivity, Thermodynamic, Conditional Stability Constants, and Kinetic Stability Data of Gadopiclenol and Other Commercial Gadolinium Chelates

International Nonproprietary Name	Gadopiclenol	Gadoterate (Meglumine Salt)		Gadobutrol	Gadoteridol	Gadobenate (Dimeglumine Salt)		Gadodiamide	Gadopentetate (Dimeglumine Salt)
		Dotarem	Gadovist, Gadavist			ProHance	MultiHance		
Trade Name	NA								
Osmolality at 37°C (mOsm/kg H <sub>2</sub> O) at marketed concentration	843*	1350†	1603†	630†	1970†	789†	1960†		
Log <i>P</i> (Octanol/PBS for gadopiclenol, Butanol/H <sub>2</sub> O for others)	-4.2*	-2.87†	-2†	-1.98†	-2.33†	-2.13†	-3.16†		
Viscosity at 37°C (mPa·s) (0.5 M except gadobutrol at 1.0 M)	7.6*	2†	4.96†	1.3†	5.3†	1.4†	2.9†		
Relaxivity (r <sub>1</sub> /r <sub>2</sub> ) mM <sup>-1</sup> s <sup>-1</sup> at 37°C	12.5/14.6* 13.2/15.1*	3.4/4.1† 4.3/5.5†§	3.7/5.1† 6.1/7.4†§	3.1/3.7† 4.8/6.1†§	4.2/4.8† 9.2/12.9†§	3.5/3.8† 4.4/4.6†§	3.4/4.0† 3.8/4.1†§		
1.5 T	12.2/15*¶ 12.8/15.1*¶	2.9/3.2† 3.6/4.3†§	3.3/3.9† 5.2/6.1†§	2.9/3.2† 4.1/5.1†§	4/4.3† 6.3/8.7†§	3.3/3.6† 4.3/5.2†§	3.3/3.9† 4.1/4.6†§		
3 T	11.3/13.5* 11.6/14.7	2.8/3.3† 3.5/4.9†§	3.2/3.9† 5/7.1†§	2.8/3.4† 3.7/5.7†§	4/4.7† 5.5/11.0†§	3.2/3.8† 4/5.6†§	3.1/3.7† 3.7/5.2†§		
Log K <sub>therm</sub>	18.7	25.6†	21.8†	23.8†	22.6†	16.9†	22.1†		
Log K <sub>cond</sub> (pH 7.4)	15.5*	19.3†	14.7†	17.1†	18.4†	14.9†	17.7†		
Kinetic stability in acidic conditions (HCl, pH 1.2) and 37°C	20 ± 3 days*	4 ± 0.5 days*	18 h†	4 h†	NA	<5 s†	<5 s†		

\*Guerbet measurements.

†Port et al (2008).<sup>12</sup>

‡Rohrer et al (2005).<sup>27</sup>

§In bovine plasma.

||In human serum.

¶Measured at 1.41 T.

NA indicates not available; PBS, phosphate buffered saline.

**TABLE 2.** Successive Protonation Constants of Gadopicolenol Ligand (Noted LH<sub>4</sub>) at 25°C in NMe<sub>4</sub>Cl Medium (0.1 mol/L)

Corresponding Chemical Equilibrium	Log K <sub>prot</sub>
L <sup>4-</sup> + H <sub>3</sub> O <sup>+</sup> ⇌ LH <sup>3-</sup> + H <sub>2</sub> O	10.57
LH <sup>3-</sup> + H <sub>3</sub> O <sup>+</sup> ⇌ LH <sub>2</sub> <sup>2-</sup> + H <sub>2</sub> O	5.99
LH <sub>2</sub> <sup>2-</sup> + H <sub>3</sub> O <sup>+</sup> ⇌ LH <sub>3</sub> <sup>-</sup> + H <sub>2</sub> O	4.06
LH <sub>3</sub> <sup>-</sup> + H <sub>3</sub> O <sup>+</sup> ⇌ LH <sub>4</sub> + H <sub>2</sub> O	2.07

in dogs, and 0%–0.1% in humans), and was also independent of the concentration.

## DISCUSSION

Gadopicolenol is a new nonspecific macrocyclic GBCA that was designed to exhibit both high relaxivity and high kinetic inertness. Its low-molecular-weight structure and lack of interaction with plasma proteins enable its use for several clinical indications including CNS and breast cancer.

The finding that linear GBCAs are associated with NSF and Gd retention at CNS sites has sparked new interest in alternative MRI contrast agents. Possible options include iron oxide nanoparticles (NPs), iron chelates, or manganese (Mn)-based contrast agents.<sup>32–34</sup> Acute and subacute toxicity data are still needed to estimate the safety profile of iron chelates.<sup>33</sup> Iron oxide NPs and Mn-based agents have been the subject of considerable research, and are not yet in clinical use for safety, regulatory, economic, or industrial reasons.<sup>35</sup>

The molecular structure of gadopicolenol was considered to offer the best compromise to get good stabilities (thermodynamic and kinetic), high r<sub>1</sub> relaxivity (around 2× that of currently available GBCAs), and the classical characteristics of a nonspecific non-protein-binding agent; that is, low molecular weight and favorable physicochemical properties, including high solubility and low

osmolality in water. To ensure good kinetic inertness, gadopicolenol was designed with a macrocyclic ligand structure, which is based on a parent PCTA ligand [2,2',2''-(3,6,9-triaza-1(2,6)-pyridinacyclodecaphane-3,6,9-triyl)triacetic acid] that contains a pyridine moiety in the macrocyclic polyamine backbone.<sup>36</sup> This PCTA structure theoretically permits the coordination of 2 water molecules in the so-called inner sphere. In Figure 1, the PCTA parent structure is shown in red with 7 coordinated arms to Gd<sup>3+</sup> and with the 2 water molecules that can complete the 9 coordination links of Gd<sup>3+</sup>.

The relaxation rate r<sub>1</sub> reflects the efficiency of an MRI contrast agent, and is determined by 2 factors. One is the contribution of water molecules directly linked to Gd<sup>3+</sup>, termed the inner sphere contribution, as described by the Solomon-Bloembergen-Morgan (SBM) theory. The other is the contribution of water molecules that diffuse near the Gd<sup>3+</sup> atom but without direct linkage, termed the outer sphere contribution, as described by the Freed theory.<sup>37</sup> In the SBM equation, the number of water molecules coordinated to Gd<sup>3+</sup> is directly proportional to the relaxation rate:

$$R_1(\text{IS}) = \frac{q[\text{CA}]}{[\text{H}_2\text{O}]} \frac{1}{T1_m + \tau_m} \quad \text{Equation 1}$$

where (IS) refers to the inner sphere, *q* is the hydration number (number of bound water nuclei per Gd ion), [CA] is the contrast agent concentration, [H<sub>2</sub>O] is the water molecule concentration, T1<sub>m</sub> refers to the T1 relaxation time value of the coordinated water protons, and τ<sub>m</sub> is the residence time of the water molecule in the inner sphere.<sup>6</sup>

T1<sub>m</sub> depends on field frequency, as well as on the global correlation time (τ<sub>c</sub>), which is governed by 3 main mechanisms: the rotational diffusion of the complex (1/τ<sub>r</sub>), the thermal transition of the unpaired electrons of Gd between excited and ground states (1/τ<sub>s</sub>), and the water exchange (1/τ<sub>m</sub>). The global correlation time τ<sub>c</sub> is calculated as follows:

$$\frac{1}{\tau_c} = \frac{1}{\tau_r} + \frac{1}{\tau_s} + \frac{1}{\tau_m} \quad \text{Equation 2}$$

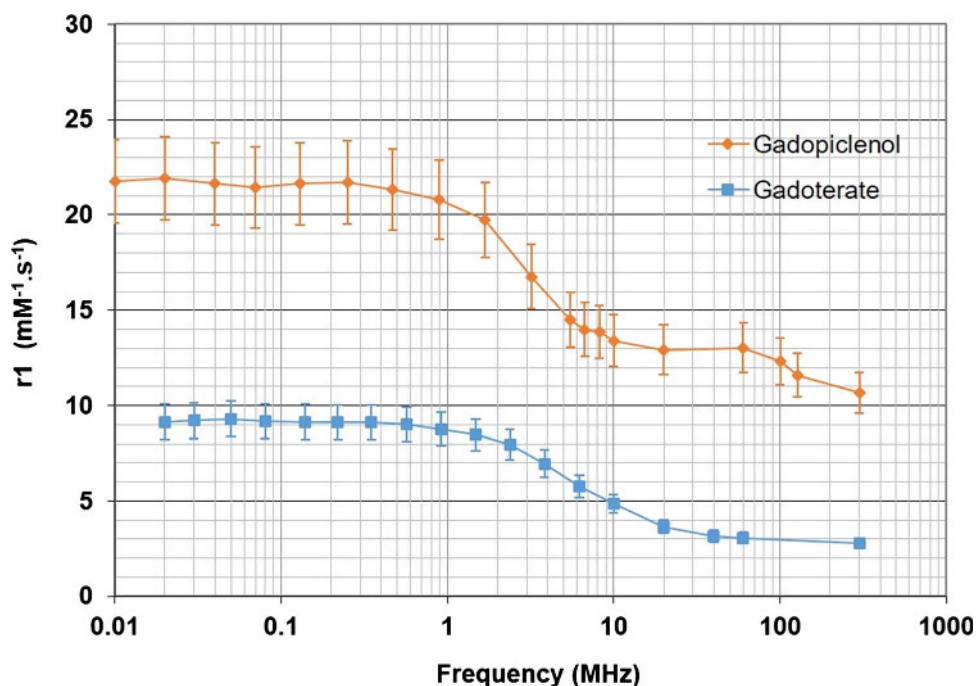


**FIGURE 2.** Nuclear magnetic relaxation dispersion profiles of gadopicolenol and gadoterate in solution with water at 37°C. Bars indicate an uncertainty of ±10% for relaxivity measurements.

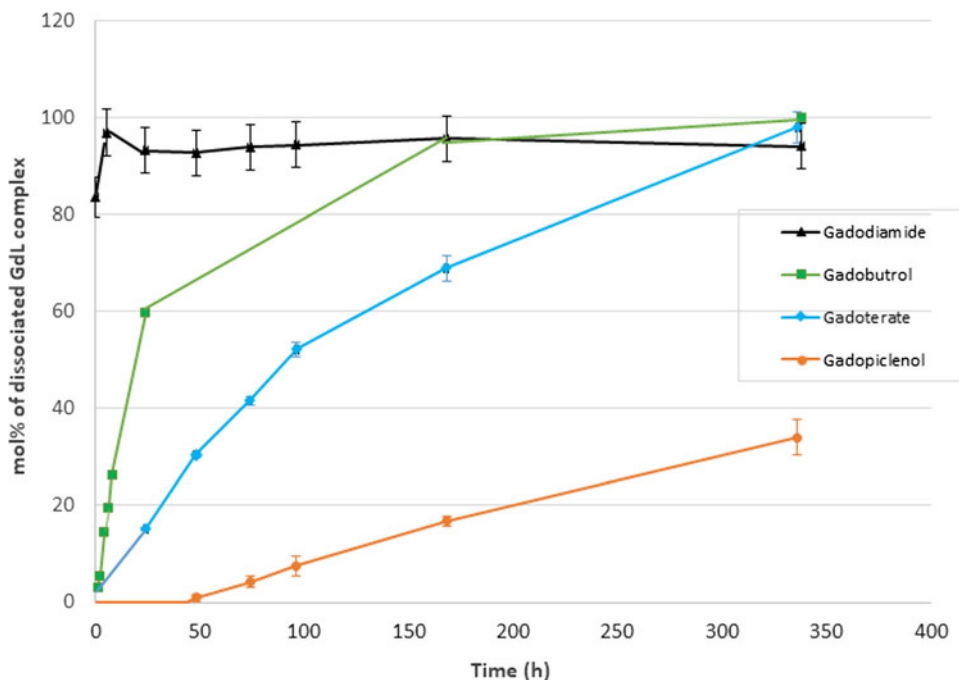


**FIGURE 3.** Dissociated  $Gd^{3+}$  (mol%) over time for gadopixelenol, gadoterate, gadobutrol, and gadodiamide under acidic conditions. The concentration of Gd chelates was  $8 \times 10^{-6}$  mol/L in HCl (pH 1.2). Measurements were performed at 37°C using Arsenazo III as the colorimetric indicator.

where  $\tau_r$  represents the rotational correlation time of the Gd chelate,  $\tau_s$  is the electronic relaxation time, and  $\tau_m$  is the lifetime of the solvent molecule in the Gd chelate.

Examining Equations 1 and 2, it is clear that the residence time should be long enough to increase the probability of relaxation but sufficiently short to allow the relaxed water molecule to undergo efficient exchange with the bulk. Equation 2 shows that of the 3 mechanisms, the fastest process will dominate. With low-molecular-weight complexes, the  $r_1$  relaxivity value is driven by the  $\tau_r$  component, since small molecules exhibit fast rotational diffusion.<sup>6</sup> Gadopixelenol was designed with small hydrophilic pendant arms to increase its global hydrodynamic size.

This reduces the rotational diffusion ( $1/\tau_r$ ), allowing  $1/\tau_s$  to be taken into account in Equation 2, and thus increasing the relaxivity according to the SBM equations. Moreover, these polyalcohol arms may increase the number of water molecules linked by the second sphere mechanism, further increasing the  $r_1$  relaxivity of gadopixelenol.<sup>38</sup>

Gadopixelenol had an  $r_1$  longitudinal relaxivity of  $11.6 \text{ mM}^{-1}\cdot\text{s}^{-1}$  in human serum at 3 T and 37°C, making it the extracellular GBCA with the highest paramagnetic effect. The NMRD profile of gadopixelenol (Fig. 2) shows its very high  $r_1$  relaxivity value up to high magnet fields ( $10.68 \text{ mM}^{-1}\cdot\text{s}^{-1}$  at 300 MHz, ie, 7 T field). This pattern is representative of Gd chelates with  $q = 2$ , which is a different type of molecular structure

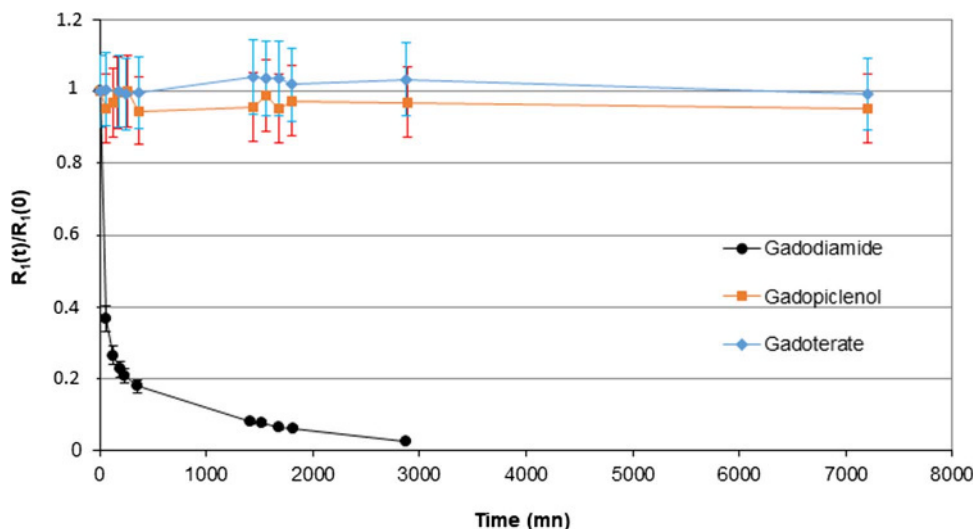


**FIGURE 4.** Temporal evolution (up to 5 days) of the  $R_1(t)/R_1(0)$  ratio for gadopixelenol, gadoterate, and gadodiamide, where  $R_1$  is the longitudinal relaxation rate. Concentration of GBCAs and  $ZnCl_2$  was 2.5 mM in phosphate buffer (pH 7.0, 335 mM). Measurements were performed at 37°C and with a field of 0.47 T.



**TABLE 3.** Results of Pharmacokinetics Studies With  $^{153}\text{Gd}$ -Gadopicolenol in Beagle Dogs (Data on 3 Males and 3 Females, Pooled)

Experimental Conditions in Dogs	
Dose, mmol Gd/kg	0.2
Number and sex of animals	6 (3 males + 3 females)
Parameters	
$t_{1/2} \beta$ , h	$0.99 \pm 0.01$
$\text{AUC}_{0-\text{inf}}$ , nmol equ·h·mL $^{-1}$	$957 \pm 77$
$\text{Cl}_t$ , mL/h/kg	$206 \pm 16$
$\text{CL}_r$ , mL/h/kg*	$179 \pm 25$
$\text{Vd}_{\text{ss}}$ , mL/kg	$239 \pm 8$

Values are given as mean  $\pm$  SD.

Slope-dependent parameters:  $\text{AUC}_{0-\text{inf}}$ ,  $t_{1/2} \beta$ ,  $\text{Cl}_t$ ,  $\text{Vd}$ ,  $\text{Vd}_{\text{ss}}$ , calculated using data to 8 hours. Renal clearance was calculated using plasma and urine values over 6 hours.

\* $n = 5$  dogs, one female dog excluded from calculation of renal clearance due to unreliable urinary excretion data.

$t_{1/2} \beta$  indicates the apparent terminal elimination half-life; AUC, area under the curve;  $\text{Cl}_t$ , total clearance;  $\text{CL}_r$ , renal clearance;  $\text{Vd}_{\text{ss}}$ , volume of distribution at steady-state.

compared with other commercial GBCAs that are characterized by a  $q = 1$  hydration number structure.

The thermodynamic constant  $\log K_{\text{therm}}$  (at very basic pH) of gadopicolenol is of 19.7. Low values of the protonation constants of the gadopicolenol ligand (Table 2), which are in the same range as those given for PCTA,<sup>39</sup> lead to a conditional constant  $\log K_{\text{cond}}$  value at physiological pH 7.4 of 15.5. This value is in the range of currently marketed GBCAs.<sup>12</sup>

Under physiological conditions (pH 7.4), GBCAs have low dissociation rates, such that potentially released free Gd concentrations are not quantifiable within an acceptable experimental time. Therefore, experiments to assess and compare the kinetic stabilities of GBCAs are conventionally performed under acidic conditions, in the presence of HCl (pH 1.2) and at 37°C, where dissociation rates are faster.<sup>12</sup> Gadolinium chelate dissociation, mediated by either spontaneous

or proton-assisted mechanisms,<sup>12</sup> is a pseudo-first-order reaction. The dissociation rate is calculated by the following equation:

$$-\frac{d[\text{GdL}]}{dt} = k_{\text{obs}} \times [\text{GdL}]. \quad \text{Equation 3}$$

where  $[\text{GdL}]$  is the Gd chelate concentration, and  $k_{\text{obs}}$  is the dissociation constant. Using this equation, the dissociation constant may be graphically determined by plotting  $\ln([\text{GdL}]_0 - [\text{Gd}^{3+}])$  as a function of time. The half-life time for Gd chelate dissociation ( $t_{1/2}$ ) can be calculated as follows:

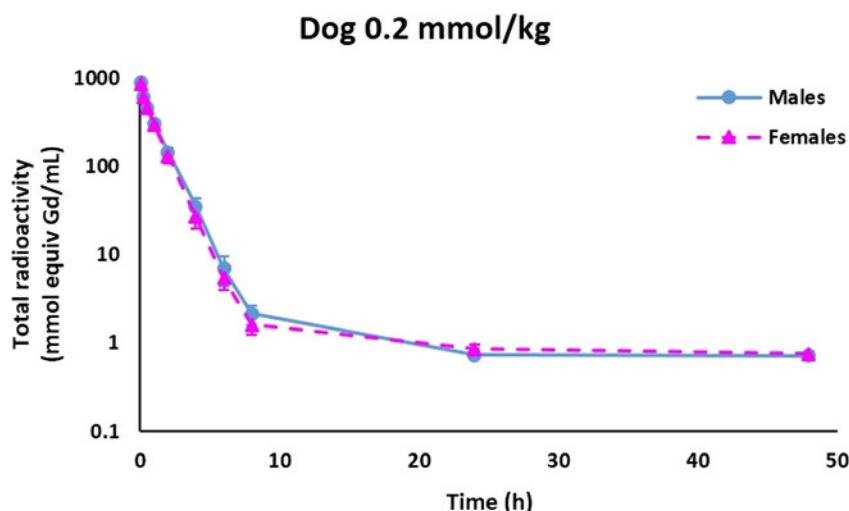
$$t_{1/2} = \frac{\ln(2)}{k_{\text{obs}}}. \quad \text{Equation 4}$$

The model relevance, as well as the dissociation behavior of gadoterate and gadodiamide, has been discussed elsewhere.<sup>12</sup>

The dissociation curves obtained at pH 1.2 (Fig. 3) demonstrate that the dissociation rates of the Gd chelates were highly dependent on the structural nature of the GBCA ligand. Under our experimental conditions, gadodiamide dissociation was almost immediate, and did not enable determination of  $k_{\text{obs}}$  and  $t_{1/2}$  values. Compared with the linear GBCA gadodiamide, macrocyclic Gd chelates (gadobutrol and gadoterate) exhibited considerably longer dissociation half-lives. Of all tested GBCAs, gadopicolenol had the longest dissociation half-life, suggesting a very high kinetic stability.

Several parameters are likely to contribute to this property. First, gadopicolenol is characterized by high conformational rigidity, similar to currently available macrocyclic GBCAs.<sup>40,41</sup> Second, the addition of substituted arms to the ligand structure introduces an additional steric constraint, thus further enhancing the ligand's conformational rigidity.

Gd chelates can interact with both endogenous ligands (eg, phosphate) and endogenous metals (eg,  $\text{Zn}^{2+}$ ,  $\text{Ca}^{2+}$ , and  $\text{Fe}^{2+/3+}$ ), as shown in various in vitro and in vivo models.<sup>42-49</sup> The clinical relevance of such models has been discussed elsewhere.<sup>17,50-52</sup> In vitro relaxivity measurements have been conducted to assess the potential dechelation reaction of gadopicolenol in the presence of phosphate and the endogenous cation  $\text{Zn}^{2+}$ . These experiments were performed under sensitized conditions to enable measurement of putative Gd dechelation, using a high-concentration phosphate buffer with an equimolar mixture of GBCAs

**FIGURE 5.** Mean ( $\pm$ SD) levels of total radioactivity in plasma plotted versus time following intravenous bolus administration of  $^{153}\text{Gd}$ -gadopicolenol (0.2 mmol Gd/kg) to Beagle dogs (3 males and 3 females).

(gadopiclesol, gadoterate, and gadodiamide) and endogenous cations ( $Zn^{2+}$ ). Under these conditions, the following reaction may occur:



where M is a divalent cation ( $Zn^{2+}$ ) that exchanges with  $Gd^{3+}$  in the chelate, and  $PO_4^{3-}$  is a phosphate anion that forms a precipitate with  $Gd^{3+}$ . In the presence of  $Zn^{2+}$  and  $PO_4^{3-}$ , the  $R_1(t)/R_1(t_0)$  ratio for gadodiamide sharply decreased, suggesting dechelation followed by precipitation of  $GdPO_4$ . Conversely, the  $r_1$  relaxivities of gadopiclesol and gadoterate remained constant over the experimental time in the presence of  $Zn^{2+}$  and  $PO_4^{3-}$ , reflecting these complexes' stability toward dechelation in the presence of phosphate and  $Zn^{2+}$ .

Osmolality of the gadopiclesol solution is among the lowest among GBCAs. The low volume administered during an MR examination should preclude physiological consequences of osmolality (because of a low osmotic load<sup>12</sup>) and viscosity of the bolus.

A molecule's octanol-water (or PBS) partition coefficient is a relevant and widely used measure of its hydrophilicity/lipophilicity ratio.<sup>53</sup> Log *P* value (measured in a 50/50 mixture of *n*-octanol and pH 7.4 phosphate-buffered saline) is consistent with a high hydrophilic structure. Direct comparison with log *P* values of other GBCAs (measured in butanol/water) is not possible.

The nonclinical pharmacokinetics investigations were performed in dogs using <sup>153</sup>Gd-labeled gadopiclesol. Since only the radioactivity is detected in such experiments, radio-HPLC was used to verify that the <sup>153</sup>Gd-gadopiclesol ratio exactly represented the bulk material, as recommended.<sup>54</sup> The distribution volume was consistent with gadopiclesol distribution within the extracellular water compartment: distribution volume at steady state ( $239 \pm 8$  mL/kg) was very similar to the extracellular fluid volume measured by the ferrocyanide method in dogs ( $237 \pm 27$  mL/kg).<sup>55</sup> Twenty-four hours after administration of gadopiclesol, almost all the injected dose was found to be excreted mostly in urine. No metabolites were found, no plasma protein binding was evidenced, and no sex-related effects were identified. Overall, the results demonstrated that gadopiclesol pharmacokinetics parameters were very similar to those of other extracellular and nonspecific GBCAs.<sup>56</sup>

Fries et al<sup>57</sup> performed a study in rats, comparing the signal-to-noise ratios of hepatic colorectal metastases and of healthy hepatic parenchyma, lesion enhancement, and contrast-to-noise ratio for gadopiclesol and gadobutrol (both intravenously injected at 0.1 mmol Gd/kg) at 9.4 T. They reported significantly better lesions enhancement with gadopiclesol compared with gadobutrol. Indeed, the current advent of MRI systems operating at high and ultra-high magnetic fields opens new avenues in neuroradiology.<sup>4,58</sup> Importantly, the high relaxivity of gadopiclesol in high fields overcomes the issues associated with the low relaxivity of currently available GBCAs in high fields.

Gd-enhanced MRI is crucial for the detection of small metastases<sup>2,4,59</sup> and further allows the distinction of metastases from nontumor white matter lesions.<sup>2</sup> Several clinical studies show benefits associated with using higher doses of GBCAs. Administration of an additional 0.2 mmol Gd/kg at 30 minutes after the clinical dose of 0.1 mmol Gd/kg of a nonspecific GBCA reportedly improves CNS metastasis detection and lesion conspicuity, sometimes leading to modification of the therapeutic strategy.<sup>5,60,61</sup> In addition, single administration of 0.3 mmol Gd/kg has been successfully used for the detection of CNS metastases.<sup>62</sup> The high relaxivity and stability properties of gadopiclesol support its potential use at lower doses than classic extracellular GBCAs, allowing equivalent visualization with a higher benefit/risk balance, and its potential to be administered at the current Gd dose of 0.1 mmol/kg, while providing better visualization of CNS lesions due to its very high relaxivity. This may dramatically impact patient management, for example, with regards to selection of surgical resection, stereotactic radiosurgery,

whole-brain radiation surgery, and so on.<sup>4</sup> Further, this GBCA with almost constant relaxivity and no protein binding may facilitate quantitative MRI.<sup>4</sup>

In conclusion, our present report summarized the physicochemical and pharmacokinetic profiles of gadopiclesol, a new extracellular and macrocyclic nonspecific Gd chelate that exhibits high relaxivity, no protein binding, high kinetic inertness, and a pharmacokinetic profile similar to that of other extracellular nonspecific GBCAs. Gadopiclesol is currently undergoing clinical development.<sup>63</sup>

## ACKNOWLEDGMENTS

The authors express their deep gratitude to Professors Robert N. Muller, Luce Vander Elst, and Sophie Laurent (Department of General, Organic, and Biomedical Chemistry, NMR and Molecular Imaging Laboratory, Mons University, Belgium) for the fruitful discussions on relaxivity and NMRD profiles interpretation. They are also very grateful to Drs Isabelle Déchamp, Françoise Chuburu, and Emmanuel Guillon, Reims Institute of Molecular Chemistry, CNRS UMR 7312, Reims University, France, for the fruitful discussions on thermodynamic constants. The authors thank Marie-Christine De Goltstein, Isabelle Grelet, and Monique Sabatou for the expert technical assistance and Dr Paul Kretschmer for reviewing the English version of the manuscript.

## REFERENCES

1. Van der Molen AJ. Diagnostic efficacy of gadolinium-based contrast media. In: Thomsen HS, Webb JAW, eds. *Contrast Media, Medical Radiology. Diagnostic Imaging*. Berlin/Heidelberg, Germany: Springer; 2014:181–191.
2. Fink KR, Fink JR. Imaging of brain metastases. *Surg Neurol Int*. 2013;4:S209–S219.
3. Nayak L, Lee EQ, Wen PY. Epidemiology of brain metastases. *Curr Oncol Rep*. 2012;14:48–54.
4. Runge VM, Heverhagen JT. Advocating the development of next-generation high-relaxivity gadolinium chelates for clinical magnetic resonance. *Invest Radiol*. 2018;53:381–389.
5. Ba-Ssalamah A, Nöbauer-Huhmann IM, Pinker K, et al. Effect of contrast dose and field strength in the magnetic resonance detection of brain metastases. *Invest Radiol*. 2003;38:415–422.
6. Caravan P, Ellison JJ, McMurry TJ, et al. Gadolinium(III) chelates as MRI contrast agents: structure, dynamics, and applications. *Chem Rev*. 1999;99:2293–2352.
7. Abu-Alfa AK. Nephrogenic systemic fibrosis and gadolinium-based contrast agents. *Adv Chronic Kidney Dis*. 2011;18:188–198.
8. Grobner T. Gadolinium—a specific trigger for the development of nephrogenic fibrosing dermopathy and nephrogenic systemic fibrosis? *Nephrol Dial Transplant*. 2006;21:1104–1108.
9. Marckmann P, Skov L, Rossen K, et al. Nephrogenic systemic fibrosis: suspected causative role of gadodiamide used for contrast-enhanced magnetic resonance imaging. *J Am Soc Nephrol*. 2006;17:2359–2362.
10. Broome DR. Nephrogenic systemic fibrosis associated with gadolinium based contrast agents: a summary of the medical literature reporting. *Eur J Radiol*. 2008;66:230–234.
11. Edwards BJ, Laumann AE, Nardone B, et al. Advancing pharmacovigilance through academic-legal collaboration: the case of gadolinium-based contrast agents and nephrogenic systemic fibrosis—a Research on Adverse Drug Events and Reports (RADAR) report. *Br J Radiol*. 2014;87:20140307.
12. Port M, Idée JM, Medina C, et al. Efficiency, thermodynamic and kinetic stability of marketed gadolinium chelates and their possible clinical consequences: a critical review. *Biometals*. 2008;21:469–490.
13. Sieber MA, Lengsfeld P, Frenzel T, et al. Preclinical investigation to compare different gadolinium-based contrast agents regarding their propensity to release gadolinium in vivo and to trigger nephrogenic systemic fibrosis-like lesions. *Eur Radiol*. 2008;18:2164–2173.
14. Pietsch H, Lengsfeld P, Steger-Hartmann T, et al. Impact of renal impairment on long-term retention of gadolinium in the rodent skin following the administration of gadolinium-based contrast agents. *Invest Radiol*. 2009;44:226–233.
15. Fretellier N, Bouzian N, Parmentier N, et al. Nephrogenic systemic fibrosis-like effects of magnetic resonance imaging contrast agents in rats with adenine-induced renal failure. *Toxicol Sci*. 2013;131:259–270.
16. Fretellier N, Idée JM, Dencausse A, et al. Comparative in vivo dissociation of gadolinium chelates in renally impaired rats: a relaxometry study. *Invest Radiol*. 2011;46:292–300.

17. Idée JM, Fretellier N, Robic C, et al. The role of gadolinium chelates in the mechanism of nephrogenic systemic fibrosis: a critical update. *Crit Rev Toxicol*. 2014;44:895–913.
18. Kanda T, Ishii K, Kawaguchi H, et al. High signal intensity in the dentate nucleus and globus pallidus on unenhanced T1-weighted MR images: relationship with increasing cumulative dose of a gadolinium-based contrast material. *Radiology*. 2014;270:834–841.
19. Zhang Y, Cao Y, Shih GL, et al. Extent of signal hyperintensity on unenhanced T1-weighted brain MR images after more than 35 administrations of linear gadolinium-based contrast agents. *Radiology*. 2017;282:516–525.
20. Frenzel T, Apte C, Jost G, et al. Quantification and assessment of the chemical form of residual gadolinium in the brain after repeated administration of gadolinium-based contrast agents: comparative study in rats. *Invest Radiol*. 2017;52:396–404.
21. Gianolio E, Bardini P, Arena F, et al. Gadolinium retention in the rat brain: assessment of the amounts of insoluble gadolinium-containing species and intact gadolinium complexes after repeated administration of gadolinium-based contrast agents. *Radiology*. 2017;285:839–849.
22. Robert P, Fingerhut S, Factor C, et al. One-year retention of gadolinium in the brain: comparison of gadodiamide and gadoterate meglumine in a rodent model. *Radiology*. 2018;288:424–433.
23. European Medicines Agency (EMA). EMA's final opinion confirms restrictions on use of linear gadolinium agents in body scans. November 11, 2017. Available at: [http://www.ema.europa.eu/docs/en\\_GB/document\\_library/Referrals\\_document/gadolinium\\_contrast\\_agents\\_31/European\\_Commission\\_final\\_decision/WC500240575.pdf](http://www.ema.europa.eu/docs/en_GB/document_library/Referrals_document/gadolinium_contrast_agents_31/European_Commission_final_decision/WC500240575.pdf). Accessed January 2, 2019.
24. US Food and Drugs Agency (FDA). Gadolinium-based Contrast Agents (GBCAs): Drug Safety Communication - Retained in Body; New Class Warnings. Available at: <https://www.fda.gov/Drugs/DrugSafety/ucm589213.htm>. Accessed January 2, 2019.
25. Kanal E, Maravilla K, Rowley HA. Gadolinium contrast agents for CNS imaging: current concepts and clinical evidence. *AJNR Am J Neuroradiol*. 2014;35:2215–2226.
26. Subedi KS, Takahashi T, Yamano T, et al. Usefulness of double dose contrast-enhanced magnetic resonance imaging for clear delineation of gross tumor volume in stereotactic radiotherapy treatment planning of metastatic brain tumors: a dose comparison study. *J Radiat Res*. 2013;54:135–139.
27. Rohrer M, Bauer H, Mintonovitch J, et al. Comparison of magnetic properties of MRI contrast media solutions at different magnetic field strengths. *Invest Radiol*. 2005;40:715–724.
28. Carr HY, Purcell EM. Effects of diffusion on free precession in nuclear magnetic resonance experiments. *Phys Rev*. 1954;94:630–638.
29. Meiboom S, Gill D. Modified spin-echo method for measuring nuclear relaxation times. *Rev Sci Instrum*. 1958;29:688–691.
30. Moreau J, Guillon E, Pierrard JC, et al. Complexing mechanism of the lanthanide cations  $\text{Eu}^{3+}$ ,  $\text{Gd}^{3+}$ , and  $\text{Tb}^{3+}$  with 1,4,7,10-tetrakis(carboxymethyl)-1,4,7,10-tetraazacyclododecane (DOTA)-characterization of three successive complexing phases: study of the thermodynamic and structural properties of the complexes by potentiometry, luminescence spectroscopy, and EXAFS. *Chemistry*. 2004;10:5218–5232.
31. Fournaise R, Petitfaux C. Study of formation of complexes in aqueous solutions. III. A new method for refinement of stability constants of complexes and other parameters of protometric titrations. *Talanta*. 1987;34:385–395.
32. Wesolowski JR, Kaiser A. Alternatives to GBCA: are we there yet? *Top Magn Reson Imaging*. 2016;25:171–175.
33. Tweedle MF. Science to practice: will gadolinium chelates be replaced by iron chelates in MR imaging? *Radiology*. 2018;286:409–411.
34. Boehm-Sturm P, Haeckel A, Hauptmann R, et al. Low-molecular-weight iron chelates may be an alternative to gadolinium-based contrast agents for T1-weighted contrast-enhanced MR imaging. *Radiology*. 2018;286:537–546.
35. Wang YX, Idée JM, Corot C. Scientific and industrial challenges of developing nanoparticle-based theranostics and multiple-modality contrast agents for clinical application. *Nanoscale*. 2015;7:16146–16150.
36. Aime S, Botta M, Geninatti Crich S, et al. NMR relaxometric studies of Gd(III) complexes with heptadentate macrocyclic ligands. *Magn Reson Chem*. 1998;36:S200–S208.
37. Freed JH. Dynamic effects of pair correlation functions on spin relaxation by translational diffusion in liquids. II. Finite jumps and independent T1 processes. *J Chem Phys*. 1978;68:4034–4037.
38. Botta M. Second coordination sphere water molecules and relaxivity of gadolinium (III) complexes: implication for MRI contrast agents. *Eur J Inorg Chem*. 2000;399–407.
39. Tircsó G, Kovacs Z, Sherry AD. Equilibrium and formation/dissociation kinetics of some Ln(III)PCTA complexes. *Inorg Chem*. 2006;45:9269–9280.
40. Meyer D, Schaefer M, Bonnemain B. Gd-DOTA, a potential MRI contrast agent. Current status of physicochemical knowledge. *Invest Radiol*. 1988;23:S232–S235.
41. Wang X, Jin T, Comblin V, et al. A kinetic investigation of the lanthanide DOTA chelates. Stability and rates of formation and of dissociation of a macrocyclic gadolinium (III) polyazapolycarboxylic MRI contrast agent. *Inorg Chem*. 1992;31:1095–1099.
42. Rasschaert M, Emerit A, Fretellier N, et al. Gadolinium retention, brain T1 hyperintensity, and endogenous metals: a comparative study of macrocyclic versus linear gadolinium chelates in renally sensitized rats. *Invest Radiol*. 2018;53:518–528.
43. Fretellier N, Idée J, Bruneval P, et al. Hyperphosphataemia sensitizes renally impaired rats to the profibrotic effects of gadodiamide. *Br J Pharmacol*. 2012;165:1151–1162.
44. Telgmann L, Wehe CA, Künnemeyer J, et al. Speciation of Gd-based MRI contrast agents and potential products of transmetalation with iron ions or parenteral iron supplements. *Anal Bioanal Chem*. 2012;404:2133–2141.
45. Robic C, Catoen S, De Goltstein MC, et al. The role of phosphate on Omniscan® dechelation: an in vitro relaxivity study at pH 7. *Biometals*. 2011;24:759–768.
46. Taupitz M, Stolzenburg N, Ebert M, et al. Gadolinium-containing magnetic resonance contrast media: investigation on the possible transchelation of  $\text{Gd}^{3+}$  to the glycosaminoglycan heparin. *Contrast Media Mol Imaging*. 2013;8:108–116.
47. Idée JM, Berthommier C, Goulas V, et al. Haemodynamic effects of macrocyclic and linear gadolinium chelates in rats: role of calcium and transmetalation. *Biometals*. 1998;11:113–123.
48. Cabella C, Crich SG, Corpillo D, et al. Cellular labeling with Gd(III) chelates: only high thermodynamic stabilities prevent the cells acting as 'sponges' of  $\text{Gd}^{3+}$  ions. *Contrast Media Mol Imaging*. 2006;1:23–29.
49. Laurent S, Elst LV, Copoix F, et al. Stability of MRI paramagnetic contrast media: a proton relaxometric protocol for transmetalation assessment. *Invest Radiol*. 2001;36:115–122.
50. Swaminathan S. Gadolinium toxicity: iron and ferroportin as central targets. *Magn Reson Imaging*. 2016;34:1373–1376.
51. Sieber MA, Steger-Hartmann T, Lengsfeld P, et al. Gadolinium-based contrast agents and NSF: evidence from animal experience. *J Magn Reson Imaging*. 2009;30:1268–1276.
52. Aime S, Caravan P. Biodistribution of gadolinium-based contrast agents, including gadolinium deposition. *J Magn Reson Imaging*. 2009;30:1259–1267.
53. Leo A, Hansch C, Elkins D. Partition coefficients and their uses. *Chem Rev*. 1971;71:525–616.
54. Tweedle MF. Using radiotracers to characterize magnetic resonance imaging contrast agents. *Invest Radiol*. 2002;37:107–113.
55. Zweens J, Frankena H, Rispen P, et al. Determination of extracellular fluid volume in the dog with ferrocyanide. *Pflugers Arch*. 1975;357:275–290.
56. Vogler H, Platzeck J, Schuhmann-Giampieri G, et al. Pre-clinical evaluation of gadobutrol: a new, neutral, extracellular contrast agent for magnetic resonance imaging. *Eur J Radiol*. 1995;21:1–10.
57. Fries P, Müller A, Seidel R, et al. P03277—A new approach to achieve high-contrast enhancement: initial results of an experimental extracellular gadolinium-based magnetic resonance contrast agent. *Invest Radiol*. 2015;50:835–842.
58. Balchandani P, Naidich TP. Ultra-high-field MR neuroimaging. *AJNR Am J Neuroradiol*. 2015;36:1204–1215.
59. Expert Panel on Radiation Oncology-Brain Metastases, Lo SS, Gore EM, et al. ACR Appropriateness Criteria® pre-irradiation evaluation and management of brain metastases. *J Palliat Med*. 2014;17:880–886.
60. Yuh WT, Engelken JD, Muhonen MG, et al. Experience with high-dose gadolinium MR imaging in the evaluation of brain metastases. *AJNR Am J Neuroradiol*. 1992;13:335–345.
61. Runge VM, Kirsch JE, Burke VJ, et al. High-dose gadoteridol in MR imaging of intracranial neoplasms. *J Magn Reson Imaging*. 1992;2:9–18.
62. Runge VM, Wells JW, Nelson KL, et al. MR imaging detection of cerebral metastases with a single injection of high-dose gadoteridol. *J Magn Reson Imaging*. 1994;4:669–673.
63. Hao J, Bourrinet P, Desché P. Assessment of pharmacokinetic, pharmacodynamic profile, and tolerance of gadopicleol, a new high relaxivity GBCA, in healthy subjects and patients with brain lesions (Phase I/IIa Study). *Invest Radiol*. 2019;54:396–402.